

Wavelength-swept spectral and pulse shaping utilizing hybrid Fourier domain modelocking by fiber optical parametric and erbium-doped fiber amplifiers

Kyle H. Y. Cheng,^{1,2} Beau A. Standish,³ Victor X. D. Yang,^{3,4,5,6} K. K. Y. Cheung,¹
Xijia Gu,³ Edmund Y. Lam,² and K. K. Y. Wong^{1,*}

¹Photonic Systems Research Laboratory, Department of Electrical and Electronic Engineering,
the University of Hong Kong, Hong Kong, China PRC

²Imaging Systems Laboratory, Department of Electrical and Electronic Engineering,
the University of Hong Kong, Hong Kong, China PRC

³Department of Electrical and Computer Engineering, Ryerson University, Toronto, Canada

⁴Department of Physics, Ryerson University, Toronto, Canada

⁵Division of Neurosurgery, University of Toronto, Toronto, Canada

⁶Imaging Research, Sunnybrook Health Sciences Center, Toronto, Canada

*kywong@eee.hku.hk

Abstract: We report the first Fourier domain modelocked (FDML) laser constructed using optical parametric amplifier (OPA) in conjunction with an erbium-doped fiber amplifier (EDFA), centered at ~1555nm, to the best of our knowledge. We utilize a one-pump OPA and a C-band EDFA in serial configuration with a tunable Fabry-Perot interferometer to generate a hybrid FDML spectrum. Results demonstrate a substantially better spectral shape, output power and stability than individual configurations, with decreased sensitivity to polarization changes. We believe this technique has the potential to enable several amplifiers to complement individual deficiencies resulting in improved spectral shapes and power generation for imaging applications such as optical coherence tomography (OCT).

©2010 Optical Society of America

OCIS codes: (140.3510) Lasers; fiber ; (190.4370) Non-linear optics, fibers.

References and links

1. E. J. Jung, C.-S. Kim, M. Y. Jeong, M. K. Kim, M. Y. Jeon, W. Jung, and Z. Chen, "Characterization of FBG sensor interrogation based on a FDML wavelength swept laser," *Opt. Express* **16**(21), 16552–16560 (2008).
2. D. Chen, C. Shu, and S. He, "Multiple fiber Bragg grating interrogation based on a spectrum-limited Fourier domain mode-locking fiber laser," *Opt. Lett.* **33**(13), 1395–1397 (2008).
3. L. A. Kranendonk, J. W. Walewski, S. T. Sanders, R. J. Huber, and J. G. Fujimoto, "Measurements of Gas Temperature in an HCCI Engine by Use of a Fourier-Domain Mode-Locking Laser," in *Laser Applications to Chemical, Security and Environmental Analysis*, Technical Digest (Optical Society of America, 2006), paper TuB2.
4. B. J. Vakoc, M. Shishko, S. H. Yun, W. Y. Oh, M. J. Suter, A. E. Desjardins, J. A. Evans, N. S. Nishioka, G. J. Tearney, and B. E. Bouma, "Comprehensive esophageal microscopy by using optical frequency-domain imaging (with video)," *Gastrointest. Endosc.* **65**(6), 898–905 (2007).
5. A. Mariampillai, B. A. Standish, E. H. Moriyama, M. Khurana, N. R. Munce, M. K. K. Leung, J. Jiang, A. Cable, B. C. Wilson, I. A. Vitkin, and V. X. D. Yang, "Speckle variance detection of microvasculature using swept-source optical coherence tomography," *Opt. Lett.* **33**(13), 1530–1532 (2008).
6. D. Huang, E. A. Swanson, C. P. Lin, J. S. Schuman, W. G. Stinson, W. Chang, M. R. Hee, T. Flotte, K. Gregory, C. A. Puliafito, and J. G. Fujimoto, "Optical coherence tomography," *Science* **254**(5035), 1178–1181 (1991).
7. W. Drexler, U. Morgner, F. X. Kärtner, C. Pitris, S. A. Boppart, X. D. Li, E. P. Ippen, and J. G. Fujimoto, "In vivo ultrahigh-resolution optical coherence tomography," *Opt. Lett.* **24**(17), 1221–1223 (1999).
8. T. C. Chen, B. Cense, M. C. Pierce, N. Nassif, B. H. Park, S. H. Yun, B. R. White, B. E. Bouma, G. J. Tearney, and J. F. de Boer, "Spectral domain optical coherence tomography: ultra-high speed, ultra-high resolution ophthalmic imaging," *Arch. Ophthalmol.* **123**(12), 1715–1720 (2005).
9. Y. Chen, A. D. Aguirre, P. L. Hsiung, S. Desai, P. R. Herz, M. Pedrosa, Q. Huang, M. Figueiredo, S. W. Huang, A. Koski, J. M. Schmitt, J. G. Fujimoto, and H. Mashimo, "Ultrahigh resolution optical coherence tomography of

- Barrett's esophagus: preliminary descriptive clinical study correlating images with histology," *Endoscopy* **39**(7), 599–605 (2007).
10. U. Schmidt-Erfurth, R. A. Leitgeb, S. Michels, B. Povazay, S. Sacu, B. Hermann, C. Ahlers, H. Sattmann, C. Scholda, A. F. Fercher, and W. Drexler, "Three-dimensional ultrahigh-resolution optical coherence tomography of macular diseases," *Invest. Ophthalmol. Vis. Sci.* **46**(9), 3393–3402 (2005).
 11. D. C. Adler, R. Huber, and J. G. Fujimoto, "Phase-sensitive optical coherence tomography at up to 370,000 lines per second using buffered Fourier domain mode-locked lasers," *Opt. Lett.* **32**(6), 626–628 (2007).
 12. S. H. Yun, G. J. Tearney, J. de Boer, N. Iftimia, and B. E. Bouma, "High-speed optical frequency-domain imaging," *Opt. Express* **11**(22), 2953–2963 (2003).
 13. R. Huber, M. Wojtkowski, and J. G. Fujimoto, "Fourier Domain Mode Locking (FDML): A new laser operating regime and applications for optical coherence tomography," *Opt. Express* **14**(8), 3225–3237 (2006).
 14. R. Huber, D. C. Adler, V. J. Srinivasan, and J. G. Fujimoto, "Fourier domain mode locking at 1050 nm for ultrahigh-speed optical coherence tomography of the human retina at 236,000 axial scans per second," *Opt. Lett.* **32**(14), 2049–2051 (2007).
 15. T. Klein, W. Wieser, B. R. Biedermann, C. M. Eigenwillig, G. Palte, and R. Huber, "Raman-pumped Fourier-domain mode-locked laser: analysis of operation and application for optical coherence tomography," *Opt. Lett.* **33**(23), 2815–2817 (2008).
 16. S. L. Hyung, J. J. Eun, N. S. Seung, Y. J. Myung, and S. K. Chang, "FDML wavelength-swept fiber laser based on EDF gain medium" in *IEEE 14th OptoElectronics and Communications Conference (OECC)*, paper FA5, (2009).
 17. M. Y. Jeon, J. Zhang, Q. Wang, and Z. Chen, "High-speed and wide bandwidth Fourier domain mode-locked wavelength swept laser with multiple SOAs," *Opt. Express* **16**(4), 2547–2554 (2008).
 18. K. K. Y. Wong, K. Shimizu, M. E. Marhic, K. Uesaka, G. Kalogerakis, and L. G. Kazovsky, "Continuous-wave fiber optical parametric wavelength converter with +40-dB conversion efficiency and a 3.8-dB noise figure," *Opt. Lett.* **28**(9), 692–694 (2003).
 19. M. E. Marhic, *Fiber Optical Parametric Amplifiers, Oscillators and Related Devices* (Cambridge University Press, 2007).
 20. K. K. Y. Cheung, H. Y. K. Cheng, S. Yang, Y. Zhou, and K. K. Y. Wong, "Fourier Domain Mode Locking Laser Sweeping Based On Optical Parametric Amplification," in *Optical Fiber Communication Conference* (2010) (accepted).
 21. S. K. Korotky, P. B. Hansen, L. Eskildsen, and J. J. Veselka, "Efficient phase modulation scheme for suppressing stimulated Brillouin scattering," in *Tech. Dig. International Conf. Integrated Optics and Optical Fiber Communications* (Hong Kong, 1995), pp. 110–111.
 22. M. E. Marhic, K. K. Y. Wong, and L. G. Kazovsky, "Fiber optical parametric amplifiers with linearly or circularly polarized waves," *J. Opt. Soc. Am. B* **20**(12), 2425–2433 (2003).
 23. R. Leonhardt, B. R. Biedermann, W. Wieser, and R. Huber, "Nonlinear optical frequency conversion of an amplified Fourier Domain Mode Locked (FDML) laser," *Opt. Express* **17**(19), 16801–16808 (2009).
-

1. Introduction

Recently, swept-source (SS) laser has become a standard laser configuration for sensing applications [1–3], particularly in the field of biomedical imaging [4,5]. Optical coherence tomography (OCT) [6] is an emerging imaging technique that generates cross-sectional images of biological tissue in-vivo with axial resolutions approaching histological standards (~1-10 μ m) [7–9]. Several types of OCT platforms have been developed for the purpose of improving the signal-to-noise ratio (SNR), enhancing the axial and transverse resolutions and increasing the A-scan rate to acquire faster and larger three-dimensional image sets [10,11]. Of particular interest is the technique of swept-source optical coherence tomography (SS-OCT), also called optical frequency domain imaging (OFDI), which is based on spectral interferometry [12]. A broadband laser source is optically filtered such that the wavelength that interacts with the sample is swept linearly in time. Recently, a new SS technique has been introduced to the field, namely, Fourier domain modelocking (FDML) developed by Huber *et al* [13]. In theory, it matches the fiber laser ring cavity length with the round trip time of the photons circulating in the cavity such that when one wavelength arrives at the filter, it combines with the same particular wavelength that is being generated. Therefore, different wavelengths can be continuously fed through the gain medium without substantial loss due to the rapidly tuning wavelength filter. Common filters used to sweep the optical wavelengths include piezo-electric driven Fabry-Perot interferometer [13] and polygon-grating filters [5]. Comparing with traditional SS, FDML can generate equivalent optical output power at a much lower pump power.

Semiconductor optical amplifier (SOA) has been commonly used to construct FDML SS laser due to its compact size and relatively wide bandwidth (~100nm). However, there are

several disadvantages of SOA when compared with other kinds of optical amplifiers, for example, it has relatively higher noise figure and lower gain compared with erbium-doped fiber amplifier (EDFA). Previous studies have demonstrated the use of a SOA in FDML configuration in the 1050 nm regime [14] and the possibility of using Raman amplifier [15] and EDFA [16] as gain media in the 1550nm regime. However, the results had shown limited bandwidth and power. Another study demonstrated two SOAs in a parallel configuration [17], where the bandwidth was increased. However it involved the coupling of the two paths leading to the two different SOAs, yielding power loss. An additional disadvantage with this setup was the need for an exactly equal length in the two paths. Otherwise the FDML operation would be compromised.

A plausible step would include aligning two optical amplifiers with distinctive optical characteristics such that their combined advantages would be greater than their individual performance. In this study, two distinctive optical amplifiers, specifically a fiber optical parametric amplifier (OPA), which has been shown to achieve noise figure as low as 3.8dB [18], and an EDFA are utilized to construct a hybrid FDML laser. Results demonstrate that their combined performance overcomes their individual deficiencies resulting in a laser with better spectral shape, pulse shape and polarization stability.

2. Principle and theory

This is the first study to demonstrate a hybrid FDML configuration, which utilizes two distinctly different types of optical amplifiers, as aforementioned, a one-pump OPA and a C-band EDFA, to the best of our knowledge. Fiber OPAs are based on the third-order non-linear susceptibility of glass fibers [19]. If one (or two, which depends on the actual configuration) strong pump(s) and a weak signal are fed into a fiber, an idler is generated. Signal and idler can grow together if pump power is high enough, and phase matching condition is satisfied. In other words, when an optical signal at angular frequency ω_s co-propagates in a fiber with a strong pump at ω_p , the signal is amplified and another frequency, called the idler, is generated at $\omega_i = 2\omega_p - \omega_s$. The idler contains the same modulation information as the input signal, with an inverted spectrum. The typical gain spectrum of an one-pump OPA shows a dip around the pump wavelength, while the C-band EDFA has an unevenly shaped gain spectrum from 1525nm – 1565nm. therefore it would be advantageous to complement the dip by applying the hybrid FDML technique in the cavity.

The FDML cavity is constructed similarly to a traditional ring cavity laser, but with the addition of a spool of ~8km single-mode fiber (SMF) spool for FDML operation and a tunable Fabry-Perot interferometer (TFPI) [13].

3. Experimental setup

The schematic diagrams of EDFA FDML [16] and OPA FDML [20] (also the hybrid FDML) are shown in Fig. 1 and Fig. 2 respectively.

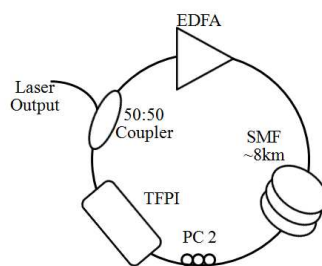


Fig. 1. Schematic diagram of EDFA FDML

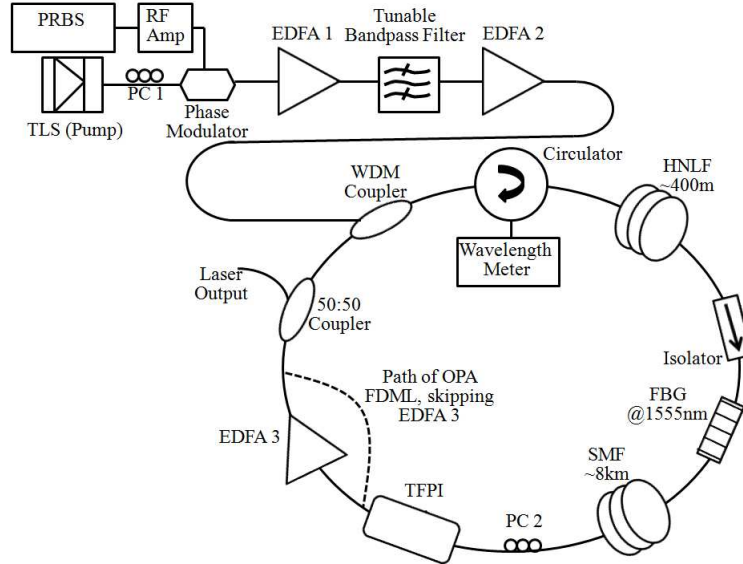


Fig. 2. Schematic diagram of the OPA FDML and hybrid FDML; the dotted line represents the path that the photons in the cavity would instead travel in the OPA FDML configuration. EDFA: erbium-doped fiber amplifier, FBG: fiber Bragg grating, HNLF: highly non-linear fiber, PC: polarization controller, PRBS: Pseudo-random Binary Sequence Generator, RF Amp: Radiofrequency Amplifier, SMF: Single Mode Fiber, TFPI: Tunable Fabry-Perot Interferometer, TLS: Tunable Laser Source, WDM Coupler: Wavelength Division Multiplexer

In Fig. 1, the EDFA FDML setup is similar to traditional FDML lasers, but with the gain medium replaced as EDFA.

The setup of the hybrid FDML configuration is depicted in Fig. 2. The pump of the OPA is depicted at the top. First, the pump wavelength was generated at $\sim 1555\text{nm}$ by the tunable laser source (TLS) which has wavelength accuracy of $\pm 0.3\text{nm}$, linewidth of 20MHz and power of 5dBm . The light then passed through a phase modulator which was modulated by a pseudo-random binary sequence (PRBS) for suppressing stimulated Brillouin scattering (SBS) [21,22]. Otherwise SBS would limit the power level that could be launched into the highly non-linear fiber (HNLF). The wavelength meter was used to monitor the SBS reflected power. Afterwards, the pump went through two stages of EDFA amplification with a tunable bandpass filter of 0.8nm bandwidth in between and then reached the HNLF for parametric amplification. The HNLF has a zero-dispersion wavelength (ZDW) of 1554nm , non-linear coefficient of $14\text{W}^{-1}\text{km}^{-1}$, a loss of $\sim 3\text{dB}$ and a dispersion slope of $0.02\text{ps/nm}^2/\text{km}$. A fiber Bragg grating (FBG) was used for attenuating the pump power in the cavity, which has -15dB reflection bandwidth of $\sim 2.5\text{nm}$ and extinction ratio of $\sim 70\text{dB}$. A sinusoidally piezo-electric driven fiber-based TFPI was used for continuously-tuned filtering, which has transmission bandwidth of $<1\text{nm}$ at each wavelength, free spectral range of $\sim 160\text{nm}$, finesse of ~ 750 and a loss of $\sim 2.5\text{dB}$. The EDFA was placed after the TFPI for the hybrid FDML generation. The $\sim 8\text{km}$ SMF fiber extended the cavity such that the round trip time of the light in the cavity was comparable to two period of the driving signal of the TFPI, which was 39.5kHz , corresponding to the second harmonic of the fundamental FDML frequency. This driving frequency was limited by the specification of the TFPI. A much higher frequency can be achieved by using a TFPI that can be driven with higher frequencies and shorter SMF (i.e. $\ll 8\text{km}$). The FDML effect could be observed by matching the sweeping period of the TFPI with half round trip time of the light in the cavity.

Previously reported OPA FDML was constructed similarly, but would follow the path depicted by the dotted line in Fig. 2. In OPA FDML, no additional EDFA was deployed into the cavity.

All the following reported spectra and pulse shapes are measured at the laser output using optical spectrum analyzer and photodetector connected to oscilloscope respectively. Each of them represents 10% of the output power.

4. Results and discussion

Spectra generated using the individual one-pump OPA and the C-band EDFA are illustrated in Fig. 3(a) [20] and Fig. 3(b), respectively.

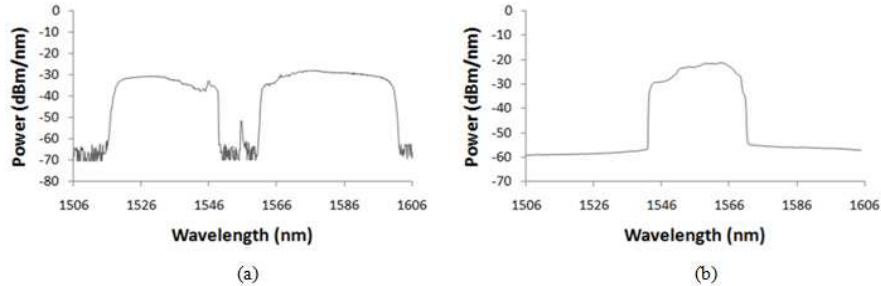


Fig. 3. (a) FDML spectrum using OPA alone, the spike at ~ 1555 nm is the pump (resolution: 0.06nm); (b) FDML spectrum using only the C-band EDFA (resolution: 0.06nm)

As shown in Fig. 3(a), OPA FDML generates a near-symmetric spectrum as expected (note that strictly speaking, the spectrum is symmetric in the frequency domain, not in the wavelength domain), with a dip in between which is consistent with the typical gain spectrum of one-pump OPA. The shorter-wavelength side of the spectrum is generated by the signal gain and the longer-wavelength side of the spectrum is generated by the idler gain. When only one side of the OPA gain spectrum is utilized, the bandwidth is ~ 30 nm. Thus it would be advantageous to complement the dip by applying the hybrid FDML technique. In Fig. 3(b), when only EDFA is utilized, it can be observed that the bandwidth in FDML configuration is insufficient for imaging or any other applications, as only ~ 20 nm of usable FDML spectrum is generated due to its uneven gain spectrum from 1525nm – 1565nm. Although the C-band EDFA has this unevenly shaped gain spectrum, it is sufficient to provide gain around the dip of the one-pump OPA. Therefore, we propose to combine these two amplifiers in the same cavity to generate a hybrid FDML effect with broadened overall operating bandwidth and better spectral shape. Figure 4 shows the FDML spectrum obtained when both one-pump OPA and C-band EDFA are utilized to generate the hybrid FDML laser. The pump power of the OPA is < 2 W. If a broader OPA spectrum is desired, pump power of the OPA can be increased and thus < 2 W is not an absolute condition in this setup. In FDML operation the both the shorter-wavelength and longer-wavelength sides of the OPA gain spectrum compensates the spectral non-uniformity of the EDFA, while the dip in the M-shaped one-pump OPA gain spectrum is partially incorporated by the EDFA gain spectrum. The amplified spontaneous emission (ASE) background is ~ 40 dB lower than peak power of the hybrid FDML output.

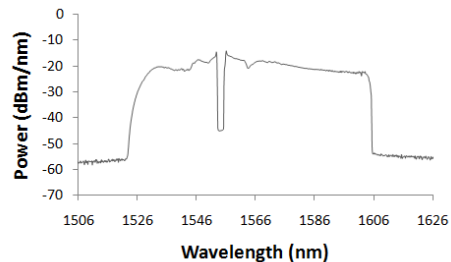


Fig. 4. Hybrid FDML spectrum (Resolution: 0.06nm)

Figure 5(a) shows the pulse waveform of the one-pump OPA FDML [20], it can be observed clearly that in both the forward and backward sweep, there is quite a large notch in the middle of each pulse. From Fig. 5(b), the pulse waveform of the hybrid FDML clearly shows a much more coherent pulse, with a slight notch which can be removed by using a FBG with smaller reflection coefficient. The resulting pulse shape is slightly more uneven because the sweeping is the result of the gain of two combined spectra. We believe that the pulse shape can be optimized by using HNLF of different ZDW and adjusting the pump wavelength, so that it can resemble a Gaussian shape, which is more suitable for OCT.

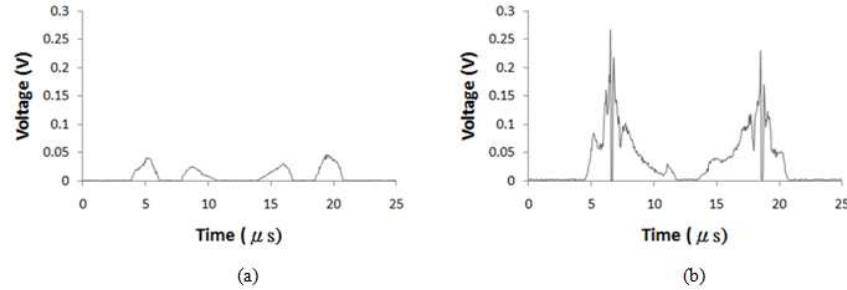


Fig. 5. (a) Pulse waveform of OPA FDML (without averaging); (b) Pulse waveform of hybrid FDML (without averaging)

The OPA FDML configuration generated output power of ~ 1.6 mW whereas the EDFA FDML generated output power of ~ 7.4 mW. The hybrid FDML configuration generated output power of ~ 85.1 mW, much higher than that of the two individual configurations, due to the combined gains of OPA and EDFA.

The instantaneous linewidth of the hybrid FDML laser was estimated to be < 0.08 nm and is comparable to standard SS laser linewidths using SOA.

The previous parallel SOA configuration was designed to generate broader bandwidth [17]. Essentially the left side of the spectrum was dominated by one SOA and the right side by another. In our design, the serial configuration showed similar performance. This is beneficial because it is much easier to setup FDML in a serial configuration.

The hybrid FDML configuration can also introduce characteristics that can complement each of the optical amplifiers. Figure 6(a) and Fig. 6(b) show the polarization sensitivity of the OPA FDML spectrum and the pulse waveform respectively by slight adjustment of the polarization controller in the cavity. However, after introducing the EDFA (EDFA 3 in Fig. 1) into the cavity, no matter how the polarization controller in the cavity is adjusted, the spectral and pulse shapes of the FDML swept-source stays relatively constant, very similar to those shown in Fig. 4 and Fig. 5(b). This also shows that cavity-based configuration with gain medium as OPA alone is very polarization sensitive. Therefore, even if a setup involving OPA is not a swept-source cavity configuration, a booster EDFA that is installed after the OPA is desirable to make a setup more polarization independent.

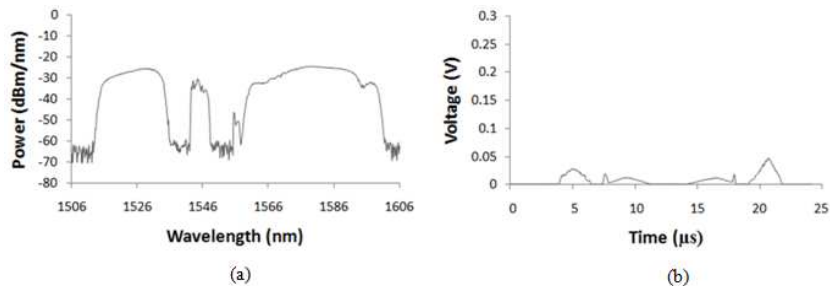


Fig. 6. (a) Distorted OPA FDML spectrum by polarization changes (resolution: 0.06nm); (b) Pulse waveform of polarization distorted OPA FDML (without averaging)

Furthermore, a one-pump OPA was used in this proof-of-principle study. Two-pump OPAs are also readily available that could be used to generate a continuous flattened spectrum with wider bandwidth [19] or even polarization independent operation [22]. The versatile gain spectrum generation at arbitrary wavelength regions of OPA may enable its incorporation into any kind of hybrid FDML configuration with any other complementary type of optical amplifiers (e.g. SOA or Raman amplifiers) further enhancing the bandwidth and/or power of existing FDML laser systems.

Previous study has also attempted to use non-linear frequency conversion to extend the bandwidth of traditional swept-source [23]. This, together with our study, demonstrate that fiber non-linear effects can potentially be used to construct next-generation swept-sources.

5. Conclusion

In conclusion, we have demonstrated a hybrid FDML laser that utilized distinct optical amplifiers to generate a FDML spectrum that combined characteristics of these amplifiers with output power of ~85.1mW. In this operation we observed significant improvements in the lasing characteristics including higher power, wider spectral bandwidth, better spectral shape and better pulse waveform when compared to the individual operation of the amplifiers. We believe that this configuration is not limited to only OPA or EDFA. Other optical amplifiers are currently being investigated (e.g. SOA or Raman amplifier) to complement individual deficiencies. Lasers with extended usable bandwidth and maximized output power are expected to be created from the hybrid FDML design for imaging use in modalities such as OCT.

We have also demonstrated that it is possible to operate in a FDML configuration through the implementation of an OPA. With the versatility of the center wavelength selection of an OPA and the wide bandwidth (possibly > 200nm), the use of an OPA in combination with additional optical amplifiers in a hybrid FDML configuration could be utilized to provide ultrahigh resolution OCT imaging.

Acknowledgment

This work was supported in part by the Research Grants Council of the Hong Kong Special Administrative Region, China under Projects HKU7179/08E and HKU7183/09E, the Canadian Foundation for Innovation, and the Canada Research Chair program. The authors would also like to acknowledge Sumitomo Electric Industries for providing the HNLF.